Stochastic Synchrony in the Olfactory Bulb

Bard Ermentrout*, Nathaniel Urban, and Roberto F. Galán

Abstract Oscillations in the 30–100 Hz range are common in the olfactory bulb (OB) of mammals. The principle neurons (mitral cells) of the OB are believed to be responsible for these rhythms. We suggest that the mitral cells, which prefer to fire in a limited range could be synchronized by receiving correlated statistically random inputs (stochastic synchrony). We explore the mechanisms of stochastic synchrony using a combination of experimental, computational and theoretical methods.

Introduction

From the earliest recordings of brain electrical signals, synchronized oscillatory activity of large populations of neurons has been seen as a prominent feature of brain activity [8]. This synchronized activity occurs in a variety of brain areas and across a wide range of frequencies. The oscillations are particularly prominent at certain areas of the brain and in certain frequency bands [9]. The vertebrate olfactory bulb [1] generates several different prominent oscillations including low-frequency oscillations that are related to respiration, and also much higher-frequency oscillations in the 30–100 Hz range. Oscillations in the range of 40–80 Hz are observed in many brain areas and are known as gamma oscillations. These signals have attracted considerable interest because of their potential role in cognitive function and/or dysfunction. Here we describe some recent work that led us to propose a novel mechanism in which synchronization in the gamma frequency band can be caused by correlations of random, noise-like fluctuations and to apply this mechanism to

B. Ermentrout (✉)
Department of Mathematics, University of Pittsburgh, Pittsburgh, PA 15260
e-mail: bard@pitt.edu

*Supported by NIMH, NSF, and NIH CRCNS

K. Josić et al. (eds.), *Coherent Behavior in Neuronal Networks*, Springer Series in Computational Neuroscience 3, DOI 10.1007/978-1-4419-0389-1_12,

the understanding of oscillatory synchrony in the mouse olfactory bulb. We also discuss the possibility that similar mechanisms may account for gamma band synchronization across other brain areas, particularly across areas that are not tightly coupled, but which may receive correlated fluctuations.

Basic Circuitry of the Olfactory Bulb Mediates Recurrent and Lateral Inhibition

The main features of main olfactory bulb circuitry are indicated in Fig. 2a, b and have been recently reviewed [16,30,48]. The principal cells of the olfactory bulb, the mitral cells, receive many excitatory inputs from olfactory receptor neurons in the nose. These inputs are made onto the highly branched tuft of the primary dendrite of the mitral cell. These cells in turn provide output to higher brain areas. Mitral cell activity is modulated by several circuits intrinsic to the bulb, most notably by dendrodendritic recurrent and lateral inhibition mediated by olfactory bulb granule cells [3, 10, 25, 49–51, 60]. These circuits are believed to refine the spatial pattern of activity across bulbar neurons [2, 59] and also are known to play an important role in altering the timing of mitral cell activity [46].

Activity of granule cells triggers release of glutamate containing vesicles in mitral cell dendrites [25, 26, 33, 43]. This glutamate binds to NMDA and AMPA receptors on the dendritic spines of postsynaptic granule cells, depolarizing them. In some cases this depolarization is localized to a particular spine, resulting in release of GABA from only that spine, back onto the mitral cell [14]. Such local release mediates a form of recurrent inhibition. In other cases, stronger depolarization may cause the granule cell to fire an action potential [15, 33] which propagates throughout the dendritic tree of the granule cell, and may cause widespread release of GABA onto the dendrites of many mitral cells. Such global activation of granule cells is believed to cause a form of lateral inhibition.

Slow Kinetics of Lateral Inhibition are Incompatible with Synchronization of Fast Oscillations

Networks coupled by recurrent and lateral inhibition have been widely studied as generators of gamma oscillations [61, 63]. However, recent physiological data, mostly from in vitro preparations [40] indicate that olfactory bulb circuitry is more complicated and more dynamic than previously believed [3, 4, 13, 24, 48, 49, 54, 60]. Of particular relevance to discussions of high-frequency oscillatory synchrony is the observation that recurrent [25, 33, 47] and lateral inhibition [61] in vitro and in vivo [33] have decay times of approximately 350 ms. These long decay times are not due to slow kinetics of individual synaptic currents, but rather because the overall IPSC is made up of a prolonged barrage of small synaptic currents, and the

rate of events in this barrage decays over several hundred milliseconds. These barrages of synaptic events are probably caused by long latency and repeated firing of olfactory bulb granule cells [27]. Each of these individual currents has a short time constant (10-ms decay) and the entire current is blocked by application of GABAA receptor antagonists. Thus, time course of granule cell-mediated inhibition spans more than 10 average gamma cycles, but is made up of many fast events. This slow time constant of lateral inhibition is incompatible with the synchronization of gamma oscillations [11, 61, 62]. However, we have described and propose further study of a mechanism whereby the fast fluctuating divergent outputs from single granule cells to multiple mitral cells provides a mechanism for synchronizing fast oscillations in mitral cells. To understand the mechanisms that may lead to this synchronization, we consider the known properties of olfactory bulb neurons and circuits.

Gamma Oscillations are Intrinsic to Olfactory Bulb and to Mitral Cells

Gamma oscillations have been observed in recordings from the olfactory bulb for many years [1, 41]. These oscillations can be readily observed by field potential recordings both in awake behaving and in anaesthetized animals [39, 53]. In vivo recordings in anaesthetized animals in which connections from cortex to the olfactory bulb were severed have shown that olfactory bulb gamma oscillations are generated intrinsically in the bulb, not requiring feedback connections from cortex [39]. These oscillations do depend on inhibition as they are not seen during pharmacological blockade of GABAA receptors and they are altered by genetic manipulation of GABAA receptors [41]. Recent work has further shown that gamma frequency oscillation can even be induced in acute olfactory bulb slices [18, 29] clearly indicating that they can be generated by the intrinsic bulbar circuitry [18,29]. This in vitro synchronization is prevented by blockade of GABAA receptors [29], and also of gap junctions, sodium current, and glutamate receptors [18].

Mitral Cells are Oscillators with a Preferred Frequency of 40 Hz

The biophysical properties of mitral cells have been investigated in detail in recent years. Mitral cells tend to have rather depolarized resting membrane potentials (−50 to −60 mV) and fire rather narrow action potentials (1-ms half width). Subthreshold current steps generate 25–50 Hz oscillations of subthreshold membrane potential in mitral cells [12] indicating that these cells have subthreshold resonance in the low gamma frequency range. Further depolarization by current steps of moderate amplitude result in long slow depolarizations which eventually generate high-frequency spiking [5]. These periods of spiking are interrupted by pauses that last hundreds of

milliseconds, during which subthreshold oscillations in the membrane potential are again observed [12]. Increasing the amplitude of the current step results in shorter pauses in firing without a large effect on the frequency of firing during the spiking period [5]. Thus, increasing the amplitude of DC current injection causes a change in the average firing rate without much change in the most common interspike interval [5]. A similar phenomenon has been observed during in vivo whole cells recordings. In these recordings, many mitral cells show fluctuations in membrane potential that track the respiration cycle, which occurs in the theta frequency range (2–5 Hz) [33]. When these cells fire action potentials, these spikes generally occur during the peak of the theta cycle. A single theta cycle can be associated with multiple spikes and these spikes occur with an instantaneous frequency of approximately 40 Hz, independent of whether the cell fire as few as 2 or as many as 6 spikes in the single theta cycle. Thus a tripling of the average firing rate can occur even when the spikes that are generated have an interspike interval of 25 ms.

These observations show that individual mitral cells are strongly biased to fire in the gamma frequency range and that firing in this frequency range occurs across a wide range of steady state current values and/or a wide range of in vivo input strengths. Given that cells with similar firing rates are more easily synchronized, such dominance of gamma frequency spiking may be important for generating oscillatory synchrony across mitral cells. Our basic hypothesis is that odor inputs result in depolarization of the mitral cells and induce them to fire. Their tendency (due to intrinsic properties) to fire in a narrow frequency range (even if the inputs slowly vary) means that they can be treated as mathematical oscillators whose phase (but not frequency) is modulated by locally correlated inhibitory input from the granule cells. Interestingly, the firing rate of mitral cells does not vary much over several orders of magnitude of odor concentration when the granule cells are present [55]. Thus, we suggest that the long-lasting strong recurrent inhibition from the granule cells serves as a brake to mitral cell activity and keeps the firing rate in a restricted range. The fast correlated noisy transients that ride on the inhibition will serve to synchronize a local population of mitral cells as we will see in the next section.

Noise-Induced Oscillatory Synchrony

In the olfactory system, gamma frequency oscillations (20–80 Hz) have been observed since the earliest recordings [1] and are enhanced during certain states and olfactory behaviors [28, 44]. The mechanisms by which olfactory bulb gamma oscillations are generated and synchronized are not, however, well understood. Some fast oscillations are intrinsic to the bulb circuitry [39] even being observed in slice preparations [18, 29], suggesting that the intrinsic connectivity can give rise to synchronization. One long-standing hypothesis has been that recurrent and lateral inhibition mediated by dendrodendritic mitral cell-granule cell synapses (reviewed by [48]) are critical for the generation and synchronization, respectively, of high

frequency oscillations in the olfactory bulb [6,34,52]. According to this hypothesis, mitral cell activity leads to recurrent inhibition which in turn stops mitral cell firing for some period. Synchronization is then achieved via lateral inhibition between mitral cells. That is, when one mitral cell inhibits its own firing, it also inhibits other mitral cells. Thus, the timing of the pauses in firing will be similar across mitral cells [12, 29]. Decaying inhibition then allows resumption of firing which again evokes recurrent and lateral inhibition. Several variants of this model have been proposed to explain olfactory bulb fast field potential oscillations [28,29,35,39,42,52]. However, little direct evidence showing that this mechanism can account for synchronous fast oscillations in the olfactory system has been provided. Alteration of inhibition changes fast field potential oscillations in vivo and in vitro [18, 29, 41], but this is consistent with other mechanisms (see below).

As described above, the kinetics of lateral inhibition in the olfactory bulb find it to be inconsistent with this proposed mechanism of gamma oscillations. We then use experimental and computational approaches to investigate the possibility that the olfactory bulb is using a different mechanism to generate synchronous oscillations. Specifically, we have shown that a mechanism that has been described theoretically [38,58] but not previously applied to real oscillating neurons accounts for synchronization of fast olfactory bulb oscillations. According to this mechanism, mitral cells firing in a roughly oscillatory pattern are synchronized by correlated, but aperiodic inputs received from common granule cells. Such a mechanism of generating synchronous oscillations has not been observed experimentally in neural systems, though it may explain some previously observed phenomena [23,45].

Stochastic Synchrony

Based on the above considerations, we suppose that the mitral cells can be regarded as noisy oscillators which receive some common (and thus correlated) input from surrounding granule cells. We can now ask if this is sufficient to cause some degree of synchronization and if so, what properties of the noise, correlation, and oscillators are necessary for this synchrony. First consider N identical nonlinear oscillators sharing a common signal:

$$\frac{\mathrm{d}X_j}{\mathrm{d}t} = F(X_j) + q\Xi(t) + \sqrt{1-q^2}\Xi_j(t) \tag{1}$$

where $\Xi(t)$ is a common noise term and $\Xi_j(t)$ are independent uncorrelated noise terms. (The noise could be colored, white, Poisson, etc). We assume that $X' = F(X)$ admits a stable limit cycle oscillator. If $q = 0$, then the intrinsic uncorrelated noise will drive the oscillators apart, however, for non-zero q, there is some shared signal which could lead to partial synchrony of the oscillators. Figure 1 shows an example simulation of 50 Hodgkin–Huxley oscillators (standard HH model with $10\,\mu\mathrm{A/cm^2}$ current injected so that they oscillate regularly)

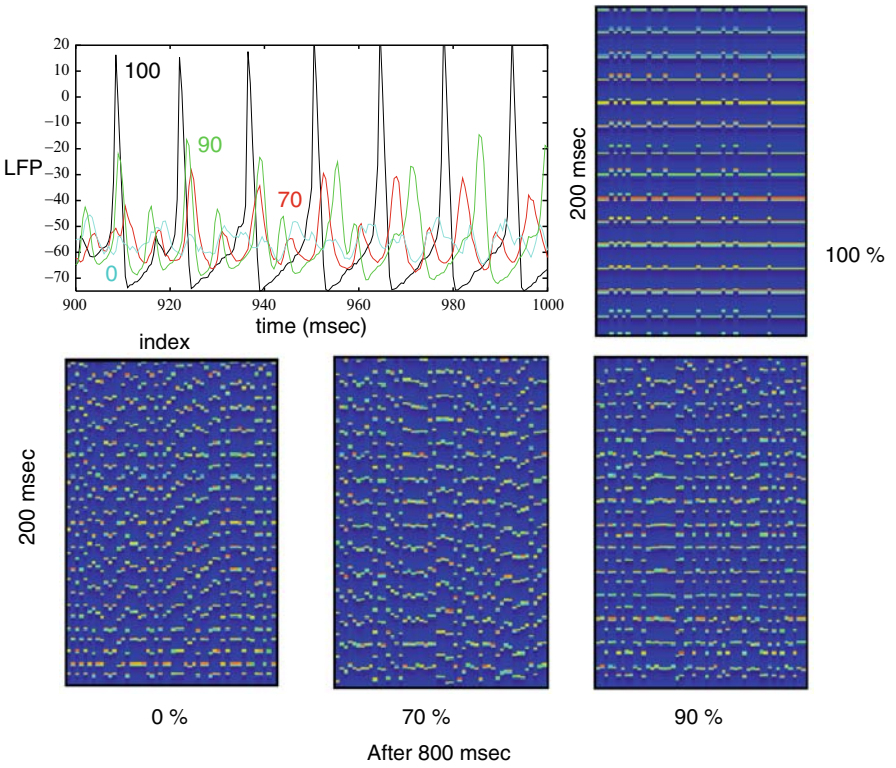

Fig. 1 Shared white noise between 50 HH oscillators. *Upper left* shows the averaged potentials of all 50 neurons as a function of the degree of correlation in the inputs. Remaining plots show potential as a function of time for these correlations.

with various values of q. The top left of the figure shows the average potential of all 50 cells: as the degree of shared input increases, a strong periodic rhythm emerges. Figure 2 shows that this behavior is not restricted to neural models. Fig. 2a, b show the underlying anatomy and membrane dynamics underlying stochastic synchrony in the olfactory bulb. In [19], we injected partially correlated input currents into a mitral cell and recorded the resulting potential. Figure 2c1 shows two trials of current injection (red and black curves) with 0% and 80% correlation. The potential traces of the mitral cells to these currents are shown in Fig. 2c2. There are clearly many more overlapping spikes when the correlation is high. To quantify this, we computed the cross-spectral density for different levels of correlation. As seen in figure 2c3,4, this grows with increased correlation and shows a peak in the 15–40 Hz range commonly found in the OB. These two figures demonstrate that common noise could play a large role in determining the synchrony between neurons.

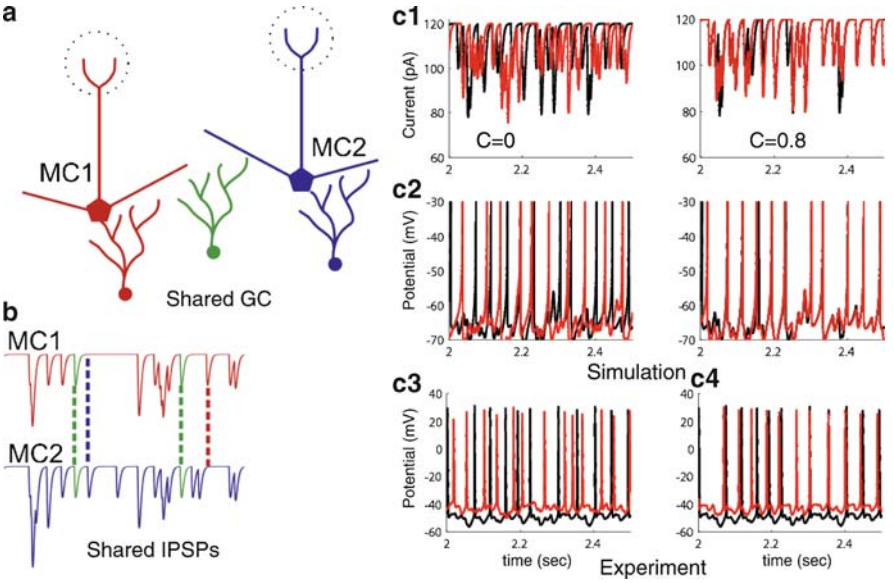

Fig. 2 Stochastic synchrony in mitral cells. (**a**) Diagram showing two uncoupled mitral cells with common granule cell; (**b**) Shared IPSPs between motral cells; (**c1**) Input currents 0% correlation and 80% correlation shown; (**c2**) Mitral cell responses to these two stimuli; (**c3**) Cross spectral density with different correlations; (**c4**) Power boost in the 15–40 Hz range due to correlation. (We depict the area under the curves in figure **c3** in the 15–40 Hz range divided by the total area under each curve.).

Phase Reduction and Lyapunov Exponents

To mathematically quantify the mechanism underlying stochastic synchrony, we apply the theory of phase reduction to (1). Since the oscillators are uncoupled and independent, we need only consider a pair of them to understand the phenomena. To consider the most general scenario, we assume that the oscillators can be slightly different and that the noise they receive is small. Furthermore, since we are interested in the role of shared currents, we assume that the only component of the oscillator which is perturbed is the somatic compartment and that the component of the vectors, Ξ, Ξ_j are ξ, ξ_j, respectively. Then, (see [58]) a pair of oscillators reduces to the pair

$$\theta_1' = \omega_1 + \Delta(\theta_1)[q\xi(t) + \sqrt{1-q^2}\xi_1(t)] \tag{2}$$

$$\theta_2' = \omega_2 + \Delta(\theta_2)[q\xi(t) + \sqrt{1-q^2}\xi_2(t)]. \tag{3}$$

In absence of stimuli, these oscillators fire at frequencies, ω_j and if the oscillators are identical, $\omega_1 = \omega_2$. The crucial function in this model is $\Delta(\theta)$, the phase

resetting curve of the oscillator. Mathematically, $\Delta(\theta)$ is proportional to the voltage component of the solution, $Y(t)$ to the linear adjoint equation:

$$Y'(t) = -D_X F(U(t))^T Y(t), \quad Y^T(t)U'(t) = 1$$

where $U'(t) = F(U(t))$ is a stable limit cycle solution. Heuristically and experimentally, $\Delta(\theta)$ is computed as follows. Let us define the phase of the oscillator to be the time since it has last produced an action potential. Thus, $0 \le \theta < P$ where P is the period of the oscillator. Suppose that we inject a brief current pulse at phase, θ of the oscillation. This will cause an action potential to occur at a time $\hat{P}$ which is not generally the same time as the time, P when it would normally occur. The phase resetting curve (PRC) for the stimulus is:

$$\mathrm{PRC}(\theta, a) = P - \hat{P}$$

where, a parameterizes the magnitude of the perturbation (for example, the total charge delivered to the neuron). The quantity, $\Delta(\theta) := \lim_{a\to 0} \mathrm{PRC}(\theta, a)/a$ defines the infinitesimal PRC or the voltage component of the adjoint.

Figure 3 shows PRCs from both model and real neurons. One point that we want to make is that there are two qualitatively different types of PRCs: those which have both a negative and positive component and those which are strictly nonnegative. The PRCs on the left have a negative and positive component.

Given the PRC, $\Delta(\theta)$, the noise, ξ_j and the heterogeneity, ω_j we can now quantify the degree of synchronization for the uncoupled pair, (2–3). Let us first assume that they are identical and the noise is completely correlated. We can ask if solutions which start near synchrony will converge to synchrony and if so, how fast they will converge. (For simplicity, we will assume that Δ has period 1 without loss of generality.) Subtract the two equations and let $\phi = \theta_2 - \theta_1$. Then for ϕ small

$$\phi' = [\Delta(\theta_1 + \phi) - \Delta(\theta_1)]\xi(t) \approx \Delta'(\theta_1)\phi\xi(t).$$

We can study how ϕ varies over time when $\xi(t)$ is white by applying Ito's lemma. Let $y = \log\phi$. Then

$$y' = -\Delta'(\theta_1)^2\frac{\sigma^2}{2} + \Delta'(\theta)\xi(t),$$

where σ^2 is the variance of the noise, $\xi(t)$. y undergoes Brownian motion with a negative drift term. Since $\phi = \exp(y)$, on average, $\phi(t)$ will decay like $\exp(\lambda t)$ where λ is the average drift:

$$\lambda = \lim_{T\to\infty} \frac{1}{T}\int_0^T -\Delta'(\theta_1(t))^2\frac{\sigma^2}{2}\,\mathrm{d}t = -\frac{\sigma^2}{2}\int_0^1 \Delta'(\theta)^2 P(\theta)\,\mathrm{d}\theta, \qquad (4)$$

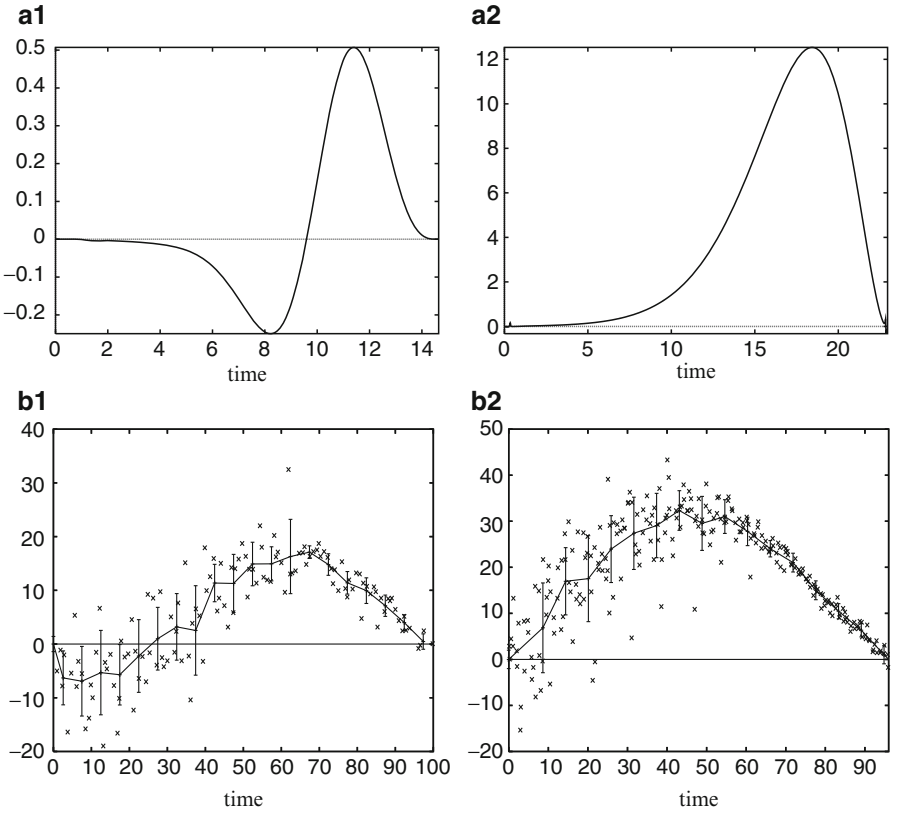

Fig. 3 Phase resetting curves. (**a1,2**) The Hodgkin–Huxley model and the Traub model with a calcium-dependent potassium current. (**b1,2**) PRCs from hippocampal neurons under different dynamic clamp scenarios. (Data provided by Theoden Netoff.)

where we have used the ergodicity of the noisy process to derive the last equality and where $P(\theta)$ is the invariant density of the phase

$$0 = -\omega \frac{\mathrm{d}P}{\mathrm{d}\theta} + \frac{\sigma^2}{2} \frac{\mathrm{d}\Delta(\theta)}{\mathrm{d}\theta} \left(\frac{\mathrm{d}\Delta(\theta) P}{\mathrm{d}\theta} \right). \tag{5}$$

If, instead of continuous noise processes, there are Poisson inputs, then the system of equations reduces to a pair of discrete maps [36]:

$$\theta_{n+1} = \theta_n + \omega \tau_n + \sigma \Delta(\theta_n)$$
$$\phi_{n+1} \approx [1 + \sigma \Delta'(\theta_n)] \phi_n,$$

where σ is the magnitude of the pulse. For this model

$$\lambda = \int_0^1 \log\left(1 + \sigma\Delta'(\theta)\right) P(\theta)\, \mathrm{d}\theta, \tag{6}$$

$$P(\theta) = \int_0^1 Q(\theta - x - \sigma\Delta(x)) P(x)\, \mathrm{d}x \tag{7}$$

where $Q(x)$ is the periodized density for an exponential distribution. Note that if σ is small, then we can expand (6) and we obtain the same equation as in (4) for the parameter λ which is called the Lyapunov exponent. In both cases, it is clearly a negative quantity, so that common noise will always cause nearby oscillators to converge to synchrony. The rate at which they converge is proportional to λ, so that more negative values of λ correspond to greater stochastic synchrony. In two papers, Tateno and Robinson [56,57] explored the Lyapunov exponent in model neurons and in cortical slices.

In recent work, Abouzeid and Ermentrout (in preparation) consider the pair of equations (4) and (5) along with a constraint

$$\int_0^1 a_0[\Delta(t)]^2 + a_1[\Delta'(t)]^2 + a_2[\Delta''(t)]^2\, \mathrm{d}t = 1$$

as an optimization problem in which one tries to minimize λ. They find using the Euler–Lagrange equations and perturbation methods that the optimal PRC is close to a sine wave, $\Delta(t) = C \sin 2\pi t$. One can also use specific parameterizations of $\Delta(t)$ which are close to the shapes of biological PRCs and then treat the optimization as a standard calculus problem. Indeed, consider $\Delta(t) = [\sin(2\pi t + a) - \sin(a)]/N(a)$ where $N(a)^2 = 3/2 - \cos(a)^2$ is chosen so the L^2 norm of $\Delta(t)$ is 1. If we assume weak noise, then $P(\theta)$ is roughly 1 and

$$\lambda \approx -\sigma^2 \frac{2\pi^2}{3 - 2\cos a}$$

which clearly has a maximum at $a = 0$. On the other hand, if we fix the square of $\Delta'(t)$ or $\Delta''(t)$ then the parameter a can be arbitrary. Similar approaches can be applied to the discrete Poisson case of equations (6) and (7). We remark that Tateno and Robinson found a similar result, PRCs with both negative and positive lobes have a more negative value for λ.

Noise Color and Reliability

Related to stochastic synchrony is the question of reliability of spikes. That is, given the same stimulus over and over again, how reliably times are the spikes of a neuron (or alternatively, how well correlated are the voltage traces). In a groundbreaking

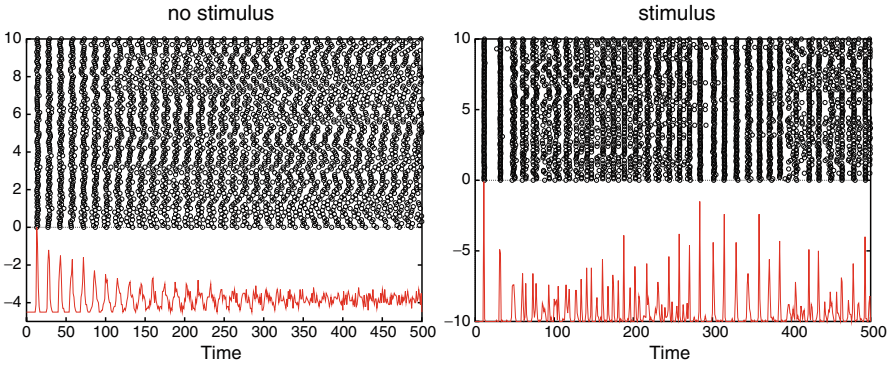

Fig. 4 Reliability in the HH model. *Left panel* shows spike rasters for 100 trials in which a constant current is applied and there is independent white noise. *Right panel* shows the same with an additional frozen noise current applied

paper, Bryant and Segundo [7] showed that a frozen white noise stimulus could produce very reliable spikes in a molluscan neuron. This was later applied by Mainen and Sejnowski [31] to cortical neurons. Figure 4 shows an example of this phenomena in the HH model. 100 trials are shown in which a constant current is applied at $t = 0$ which lasts for 500 ms. Below the spike rasters, we have binned the number of cells firing in a short time window. The initially reliable spikes degrade over time. On the other hand, if a small frozen noise signal is added on top of the constant current, then a large fraction of spikes can be reliably maintained over the duration of the stimulus. The implications for this in coding are reviewed in Ermentrout et al (2008).

We can quantify reliability as

$$R \equiv \lim_{T\to\infty} \frac{(1/T)\int_0^T s_1(t)s_2(t)\,\mathrm{d}t}{(1/T)\int_0^T s_1(t)^2\,\mathrm{d}t},$$

where $s_j(t)$ is a measure of the spike times, for example, a narrow Gaussian centered at the spike times of two signals. Note that this is like the normalized correlation. In an unpublished calculation, we show that when a stimulus is presented repeatedly in the presence of independent white noise, the reliability is related to the Lyapunov exponent:

$$R = \frac{\sqrt{-2\lambda}b}{\sqrt{-2b\lambda + \sigma_{\mathrm{E}}^2}}, \tag{8}$$

where b is a parameter related to the Gaussian smoothing of the spike times and σ_{E} is the extrinsic (independent) noise. Note that as $\sigma_{\mathrm{E}} \to 0$, $R \to 1$. Since reliability is a monotonic function of $-\lambda$, this means that the maximal reliability occurs when $-\lambda$ is largest.

Conventional wisdom is that white noise is the best stimulus for reproducible spikes. However, if the frozen noise is small and the neurons are (noisy) oscillators, then it turns out that colored noise can produce greater reliability. Galán et al. [22] demonstrate this for both real and model neurons. Equation (8) shows that the reliability is related to the Lyapunov exponent, so that we will try to calculate this in the presence of colored noise generated by the Ornstein-Uhlenbeck process:

$$\mathrm{d}\xi = -\beta\xi \mathrm{d}t + \sqrt{\beta}\mathrm{d}W,$$

where β determines the autocorrelation of the noise, $C(t) := \langle \xi(0)\xi(t)\rangle = \exp(-\beta|t|)$ and $W(t)$ is delta-correlated noise with variance, $\sigma^2/2$. Recall that the Lyapunov exponent satisfies

$$\lambda = \lim_{T\to\infty} \frac{1}{T}\int_0^T \Delta'(\theta(t))\xi(t)\,\mathrm{d}t, \tag{9}$$

where $\theta(t)$ satisfies

$$\theta'(t) = 1 + \delta(\theta(t))\xi(t). \tag{10}$$

For small noise $\sigma \ll 1$, we can approximate the phase,

$$\theta(t) = t + \int_0^t \Delta(s)\xi(s)\,\mathrm{d}s$$

and thus (9) is

$$\lambda \approx \lim_{T\to\infty} \frac{1}{T}\int_0^T \Delta''(t)\int_0^t \Delta(s)C(t-s)\,\mathrm{d}s.$$

For example, if $\Delta(\theta) = a\sin 2\pi\theta$ and $C(t) = \exp(-\beta|t|)$, then

$$\lambda \approx -K\frac{\beta}{\beta^2 + 4\pi^2}$$

where K is a positive constant dependent on the magnitude of the noise, but not β. In this case, clearly the most negative λ occurs when $\beta = 2\pi$.

Figure 5a shows that there is a clear peak in the value of reliability as a function of $\tau := 1/\beta$ for model and real neurons driven to fire at about 40 Hz. Figure 5b shows the approximate value of the Lyapunov exponent from the calculations for a sinusoidal PRC along with the values obtained from a Monte Carlo simulation. For PRCs dominated by the first Fourier mode, the rule of thumb is that the optimal time constant for colored noise is $\tau_{\mathrm{opt}} \approx P/2\pi$ where P is the period of the oscillator.

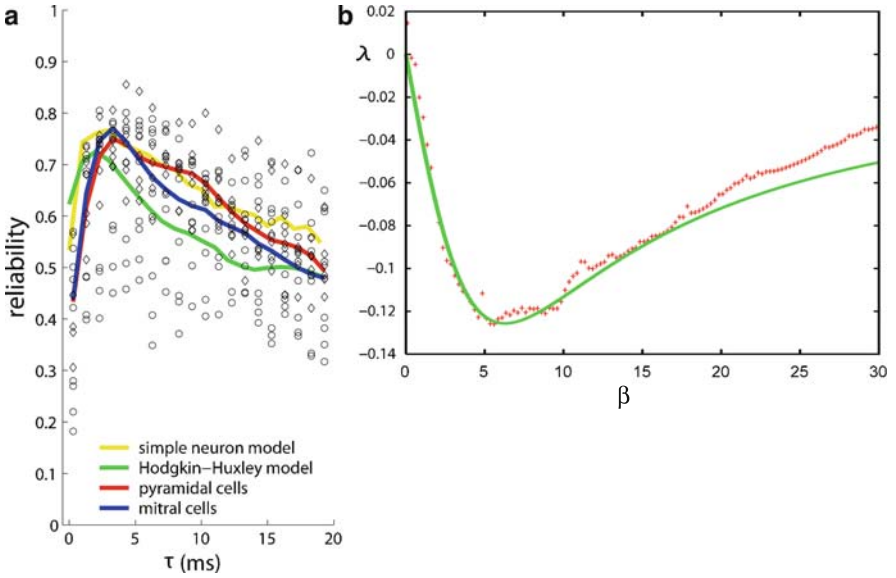

Fig. 5 Reliability as a function of the noise color. (**a**) Experiments and simulations show the peak of reliability for a 40-Hz oscillator at about 4 ms time constant. (**b**) Montecarlo and theory for a sinusoidal PRC.

Input/Output Correlations

To study the output vs. input correlations, we consider (2) and (3) where $\omega_1 = \omega_2$ but $q < 1$. Nakao et al. [37] studied this problem for white noise and Marella and Ermentrout [32] for Poisson inputs. In both cases, one is interested in the stationary density for the phase-differences between the two oscillators, that is, the random variable, $\phi := \theta_2 - \theta_1$. It turns out that through a series of perturbation expansions, one obtains the same result no matter whether the noise is white or Poisson:

$$P(\phi, c) = \frac{K}{1 - c\frac{h(\phi)}{h(0)}}, \tag{11}$$

where

$$h(\phi) = \int_0^1 \Delta(s)\Delta(s+\phi),$$

$c = 2q/(1+q)$ is the correlation, and K is a normalization so that the integral is 1. Note that as $q \to 1$, this distribution approaches a delta function corresponding to perfect synchrony. One way to characterize the degree of synchrony is the "order parameter"

$$z(c) := \int_0^1 \cos 2\pi s P(s, c)\, \mathrm{d}s$$

which is zero for a uniform P and 1 for a delta function. Another way to characterize the degree of synchrony is to look at the deviation of the peak from the uniform distribution $P(0, c) - 1$. Marella and Ermentrout [32] explore the dependence of z and other order parameters on the shape of the PRC. In particular, they examine $z(q)$ with different PRC shapes and find that if the L^2 norm of the PRC is kept constant, PRCs which have the smallest DC component maximize this function. As a final example, for small correlation, c, Marella and Ermentrout obtain a simple expression for the deviation of the peak

$$P(0, c) - 1 \approx c \left[1 - \frac{\langle \Delta \rangle^2}{\langle \Delta^2 \rangle} \right]$$

where $\langle x \rangle = \int_0^1 x(s)\, \mathrm{d}s$. If we keep the L^2 norm of the PRC constant, say 1, then the denominator is 1 and the peak deviation is maximal when Δ has zero mean – that is, no DC component.

Summary

Oscillations are ubiquitous in the nervous system and in the olfactory bulb in particular. In order for there to be large macroscopic local field potentials, there must be a good deal of synchrony in the rhythmic behavior of the principle cells, here, the mitral cells. Inhibition persists for too long and there is no direct coupling between these neurons. Thus, we have posited that a primary mechanism for synchronization is shared "noisy" inhibitory postsynaptic currents (inhibitory miniature events) from the interneurons, granule cells. We have characterized the degree of this so-called stochastic synchronization by reducing complex neuronal networks to dynamics of the phases of each neural oscillator. This has allowed us to derive some expression for the degree of synchrony as a function of properties of the noise and properties of the underlying oscillations. Furthermore, our simple theories have been put to experimental tests both in complicated membrane models and in real central nervous system neurons.

References

1. Adrian ED (1942) Olfactory reactions in the brain of the hedgehog. J Physiol 100:459–473.
2. Arevian AC, Kapoor V, Urban NN (2008) Activity-dependent gating of lateral inhibition in the mouse olfactory bulb. Nat Neurosci 11:80–87.
3. Aroniadou-Anderjaska V, Ennis M, Shipley MT (1999) Dendrodendritic recurrent excitation in mitral cells of the rat olfactory bulb. J Neurophysiol 82:489–494.
4. Aungst JL, Heyward PM, Puche AC, Karnup SV, Hayar A, Szabo G, Shipley MT (2003) Centre-surround inhibition among olfactory bulb glomeruli. Nature 426:623–629.
5. Balu R, Larimer P, Strowbridge BW (2004) Phasic stimuli evoke precisely timed spikes in intermittently discharging mitral cells. J Neurophysiol 92:743–753.

6. Bressler SL, Freeman WJ (1980) Frequency analysis of olfactory system EEG in cat, rabbit, and rat. Electroencephalogr Clin Neurophysiol 50:19–24.
7. Bryant, HL, Segundo, JP (1976) Spike initiation by transmembrane current: a white-noise analysis. J. Physiol. 260:279–314.
8. Buzsaki G (2006) Rhythms of the Brain. Oxford: Oxford University Press.
9. Buzsaki G, Draguhn A (2004) Neuronal oscillations in cortical networks. Science 304:1926–1929.
10. Carlson GC, Shipley MT, Keller A (2000) Long-lasting depolarizations in mitral cells of the rat olfactory bulb. J Neurosci 20:2011–2021.
11. Chow CC, White JA, Ritt J, Kopell N (1998) Frequency control in synchronized networks of inhibitory neurons. J Comput Neurosci 5:407–420.
12. Desmaisons D, Vincent JD, Lledo PM (1999) Control of action potential timing by intrinsic subthreshold oscillations in olfactory bulb output neurons. J Neurosci 19:10727–10737.
13. Didier A, Carleton A, Bjaalie JG, Vincent JD, Ottersen OP, Storm-Mathisen J, Lledo PM (2001) A dendrodendritic reciprocal synapse provides a recurrent excitatory connection in the olfactory bulb. Proc Natl Acad Sci USA 98:6441–6446.
14. Egger V, Svoboda K, Mainen ZF (2003) Mechanisms of lateral inhibition in the olfactory bulb: efficiency and modulation of spike-evoked calcium influx into granule cells. J Neurosci 23:7551–7558.
15. Egger V, Svoboda K, Mainen ZF (2005) Dendrodendritic synaptic signals in olfactory bulb granule cells: local spine boost and global low-threshold spike. J Neurosci 25:3521–3530.
16. Egger V, Urban NN (2006) Dynamic connectivity in the mitral cell-granule cell microcircuit. Sem Cell Develop Biol 17.
17. Ermentrout GB, Galán RF, Urban NN. (2008) Reliability, synchrony and noise. Trends Neurosci 31(8):428–434.
18. Friedman D, Strowbridge BW (2003) Both electrical and chemical synapses mediate fast network oscillations in the olfactory bulb. J Neurophysiol 89:2601–2610.
19. Galán, RF, Ermentrout, GB, Urban, NN (2005) Efficient estimation of phase-resetting curves in real neurons and its significance for neural-network modeling. Phys Rev Lett 94, 158101.
20. Galán, RF, Fourcaud-Trocme, N, Ermentrout, GB, Urban, NN (2006) Correlation-induced synchronization of oscillations in olfactory bulb neurons. J Neurosci 26, 3646–3655.
21. Galán, RF, Ermentrout, GB, Urban, NN (2007) Stochastic dynamics of uncoupled neural oscillators: Fokker-Planck studies with the finite element method. Phys Rev E Stat Nonlin Soft Matter Phys 76, 056110.
22. Galán, RF, Ermentrout, GB, Urban, NN (2008) Optimal time scale for spike-time reliability: theory, simulations and experiments. J Neurophysiol 99, 277–283.
23. Hasenstaub A, Shu Y, Haider B, Kraushaar U, Duque A, McCormick DA (2005) Inhibitory postsynaptic potentials carry synchronized frequency information in active cortical networks. Neuron 47:423–435.
24. Isaacson JS (1999) Glutamate spillover mediates excitatory transmission in the rat olfactory bulb [see comments]. Neuron 23:377–384.
25. Isaacson JS, Strowbridge BW (1998) Olfactory reciprocal synapses: dendritic signaling in the CNS. Neuron 20:749–761.
26. Jahr CE, Nicoll RA (1980) Dendrodendritic inhibition: demonstration with intracellular recording. Science 207:1473–1475.
27. Kapoor V, Urban NN (2006) Glomerulus-specific, long-latency activity in the olfactory bulb granule cell network. J Neurosci 26:11709–11719.
28. Kay LM, Laurent G (1999) Odor- and context-dependent modulation of mitral cell activity in behaving rats. Nat Neurosci 2:1003–1009.
29. Lagier S, Carleton A, Lledo PM (2004) Interplay between local GABAergic interneurons and relay neurons generates gamma oscillations in the rat olfactory bulb. J Neurosci 24:4382–4392.
30. Lowe GD, Woodward M, Rumley A, Morrison CE, Nieuwenhuizen W (2003) Associations of plasma fibrinogen assays, C-reactive protein and interleukin-6 with previous myocardial infarction. J Thromb Haemost 1:2312–2316.

31. Mainen, ZF, Sejnowski, TJ (1995) Reliability of spike timing in neocortical neurons. Science 268:1503–1506.
32. Marella, S, Ermentrout, GB (2008) Class-II neurons display a higher degree of stochastic synchronization than class-I neurons. Phys Rev E Stat Nonlin Soft Matter Phys 77, 041918.
33. Margrie TW, Sakmann B, Urban NN (2001a) Action potential propagation in mitral cell lateral dendrites is decremental and controls recurrent and lateral inhibition in the mammalian olfactory bulb. Proc Natl Acad Sci USA 98:319–324.
34. Mori K, Nowycky MC, Shepherd GM (1981) Electrophysiological analysis of mitral cells in the isolated turtle olfactory bulb. J Physiol (Lond) 314:281–294.
35. Mori K, Takagi SF (1978) An intracellular study of dendrodendritic inhibitory synapses on mitral cells in the rabbit olfactory bulb. J Physiol (Lond) 279:569–588.
36. Nagai, K et al. (2005) Synchrony of neural oscillators induced by random telegraphic currents. Phys Rev E Stat Nonlin Soft Matter Phys 71, 036217.
37. Nakao H, Arai K, Kawamura Y (2007) Noise-Induced Synchronization and Clustering in Ensembles of Uncoupled Limit-Cycle Oscillators, Phys. Rev. Lett. 98, 184101.
38. Nakao H, Arai K-S, Nagai K, Tsubo Y, Kuramoto Y (2005) Synchrony of limit-cycle oscillators induced by random external impulses. Phys Rev E 72.
39. Neville KR, Haberly LB (2003) Beta and gamma oscillations in the olfactory system of the urethane-anesthetized rat. J Neurophysiol 90:3921–3930.
40. Nickell WT, Shipley MT, Behbehani MM (1996) Orthodromic synaptic activation of rat olfactory bulb mitral cells in isolated slices. Brain Res Bull 39:57–62.
41. Nusser Z, Kay LM, Laurent G, Homanics GE, Mody I (2001) Disruption of GABA(A) receptors on GABAergic interneurons leads to increased oscillatory power in the olfactory bulb network. J Neurophysiol 86:2823–2833.
42. Powell KR, Koppelman LF, Holtzman SG (1999) Differential involvement of dopamine in mediating the discriminative stimulus effects of low and high doses of caffeine in rats. Behav Pharmacol 10:707–716.
43. Rall W, Shepherd GM, Reese TS, Brightman MW (1966) Dendrodendritic synaptic pathway for inhibition in the olfactory bulb. Exp Neurol 14:44–56.
44. Ravel N, Chabaud P, Martin C, Gaveau V, Hugues E, Tallon-Baudry C, Bertrand O, Gervais R (2003) Olfactory learning modifies the expression of odour-induced oscillatory responses in the gamma (60-90 Hz) and beta (15-40 Hz) bands in the rat olfactory bulb. Eur J Neurosci 17:350–358.
45. Reyes AD (2003) Synchrony-dependent propagation of firing rate in iteratively constructed networks in vitro. Nat Neurosci 6:593–599.
46. Schaefer AT, Angelo K, Spors H, Margrie TW (2006) Neuronal Oscillations Enhance Stimulus Discrimination by Ensuring Action Potential Precision. PLoS Biol 4:e163.
47. Schoppa NE, Kinzie JM, Sahara Y, Segerson TP, Westbrook GL (1998) Dendrodendritic inhibition in the olfactory bulb is driven by NMDA receptors. J Neurosci 18:6790–6802.
48. Schoppa NE, Urban NN (2003) Dendritic processing within olfactory bulb circuits. Trends Neurosci 26:501–506.
49. Schoppa NE, Westbrook GL (2001a) Glomerulus-specific synchronization of mitral cells in the olfactory bulb. Neuron 31:639–651.
50. Schoppa NE, Westbrook GL (2001b) NMDA receptors turn to another channel for inhibition. Neuron 31:877–879.
51. Schoppa NE, Westbrook GL (2002) AMPA autoreceptors drive correlated spiking in olfactory bulb glomeruli. Nat Neurosci 5:1194–1202.
52. Segev I (1999) Taming time in the olfactory bulb. Nat Neurosci 2:1041–1043.
53. Singer W, Gray C, Engel A, Konig P, Artola A, Brocher S (1990) Formation of cortical cell assemblies. Cold Spring Harb Symp Quant Biol 55:939–952.
54. Smith TC, Jahr CE (2002) Self-inhibition of olfactory bulb neurons. Nat Neurosci 5:760–766.
55. Stopfer M, Jayaraman V, Laurent G. (2003) Intensity versus identity coding in an olfactory system. Neuron 39:991–1004.
56. Tateno T, Robinson HP (2007a) Quantifying noise-induced stability of a cortical fast-spiking cell model with Kv3-channel-like current. Biosystems 89(1-3):110–116.

57. Tateno T, Robinson HP (2007b) Phase resetting curves and oscillatory stability in interneurons of rat somatosensory cortex. Biophys J 92(2):683–695.
58. Teramae JN, Tanaka D (2004) Robustness of the noise-induced phase synchronization in a general class of limit cycle oscillators. Phys Rev Lett 93:204103.
59. Urban NN (2002) Lateral inhibition in the olfactory bulb and in olfaction. Physiol Behav 77:607–612.
60. Urban NN, Sakmann B (2002) Reciprocal intraglomerular excitation and intra- and interglomerular lateral inhibition between mouse olfactory bulb mitral cells. J Physiol 542:355–367.
61. Wang XJ, Buzsaki G (1996) Gamma oscillation by synaptic inhibition in a hippocampal interneuronal network model. J Neurosci 16:6402–6413.
62. White JA, Chow CC, Ritt J, Soto-Trevino C, Kopell N (1998) Synchronization and oscillatory dynamics in heterogeneous, mutually inhibited neurons. J Comput Neurosci 5:5–16.
63. Whittington MA, Traub RD, Kopell N, Ermentrout B, Buhl EH (2000) Inhibition-based rhythms: experimental and mathematical observations on network dynamics. Int J Psychophysiol 38:315–336.